A robust dipole moment of carbon monoxide (CO) is a permanent puzzle for both spectroscopic and *ab initio* studies

Vladimir V. Meshkov, Elena A. Pazyuk & Andrey V. Stolyarov

View supplementary material

Published online: 19 Nov 2024.

Submit your article to this journal

Article views: 233

View related articles

View Crossmark data

Taylor & Francis
Taylor & Francis Group

ALEXANDER NEMUKHIN SPECIAL ISSUE (BY INVITATION ONLY)

Check for updates

A robust dipole moment of carbon monoxide (CO) is a permanent puzzle for both spectroscopic and *ab initio* studies

Vladimir V. Meshkov, Elena A. Pazyuk and Andrey V. Stolyarov

Department of Chemistry, Lomonosov Moscow State University, Moscow, Russia

ABSTRACT

The asymptotically correct semi-empirical dipole moment function (DMF) for the ground $X^1\Sigma^+$ state of the CO molecule was redetermined in an analytical form for the entire range of interatomic distances $r \in [0, +\infty]$ by a global least-squared fitting both experimental intensities and *ab initio* data. The region $r \in [0.8, 1.9]$ Å that is governed exclusively by the empirical data was broadened by adding experimental relative intensity ratios measured in the emission from high vibrational levels v. Absolute absorption intensities recently obtained for very high 7-0 overtone and accompanied sub-percent measurements for 3-0 band were also included in the fitting procedure. The present DMF reproduces a vast majority of the experimental intensities up to $v \leq 38$ within accuracy of measurements, except 'abnormally' sensitive 5-0 band, and systematically overestimates the most previous *ab initio* and semi-empirical functions at $r \geq 1.5$ Å. Possible reasons of the observed discrepancies are throughout discussed. The resulting DMF can be used, along with mass-invariant interatomic potential, to upgrade rovibrational line lists for any isotopologues of the CO molecule up to the dissociation threshold. The corresponding FORTRAN subroutine is provided.

1. Introduction

Carbon monoxide (CO) is one of the most important components in atmospheric and astrophysical studies [1–9], being the environmental pollutant and the second (after H_2) most common molecule in the observable Universe. Numerous numbers of high resolution spectroscopic measurements of line positions and absolute absorption intensities on naturally abounded isotopologues of CO [10–12] have been combined with the accurate *ab initio* electronic structure calculations through a global Direct-Fit-Method [13] that consolidates them into the mass-invariant interatomic potential energy curve (PEC) [14,15] and dipole moment function (DMF) [16–18], enabling predictions on the energy and radiative properties for a vast majority of rovibrational transitions in the ground $X^1\Sigma^+$ state of CO isotopologues with the almost experimental (sometimes, even sub-percent) accuracy [19–21].

It is a common place that a strong complementary interlink between the experimental and theoretical approaches is inevitably required to provide the most robust structure and dynamics of quantum systems [22]. The state-of-art accuracy of both spectroscopy

measurements [23–25] and *ab initio* calculations [24,26–28] systematically increase, however, the derived experimental and theoretical results can still unacceptably diverge from each other. The permanent DMF for the ground state of the CO molecule belongs to this case, despite the last decade of extensive semi-empirical DMF studies [16–18,29]. The particular challenge arises from the limitation that while the CO ground state mass-invariant semi-empirical PEC has been accurately determined for vibrational levels up to $v = 41$ [15], the corresponding DMF has been still reconstructed, with the acceptable accuracy, for only the lowest vibrational levels $v \leq 7$ [27], covering a narrow interval of interatomic distances from approximately 0.9 to 1.5 Å.

On the theoretical side, the DMF behaviour was recently *ab initio* investigated near the equilibrium area ($0.8 < r < 1.5$ Å) using single-reference coupled-cluster methods up to the CCSDT level, taking into account relativistic and quantum-electrodynamics (QED) effects [28,30]. The long-range region ($r > 5.5$ Å) of the DMF and PEC was also thoroughly examined using a multi-reference configuration interaction (CISD) approach [31]. Additionally, several multi-reference CI and the
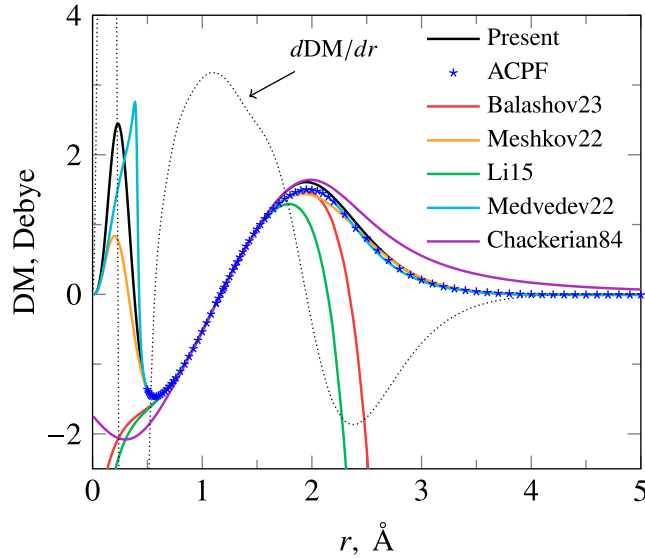

Figure 1. The overview of permanent dipole moment functions available for the ground state of CO molecule. *Ab initio* points were calculated using the MR-ACPF method in Ref. [17] while other functions borrowed from Ref's. [16–18,27,34]. Note, that the current DMF is defined as positive for the polarity C^+O^- in this work.

averaged coupled-pair functional (ACPF) studies should be mentioned for their valuable contributions to this area [16,17,27,32,33]. The most robust MR-CI and MR-ACPF results [17] available over a large range of interatomic distances clearly demonstrate the 'unusual' undulating behaviour of the CO DMF, which has exactly three non-trivial roots (see, Figure 1) on the semi-interval $r \in [0, +\infty]$. The second root is located in vicinity of the equilibrium point $r_e \approx 1.13$ Å, leading to the rather weak rotational transitions. At the same time, the corresponding maximum of the 1-st derivative of the DMF with respect to r yields intensive vibrational transitions.

In the present work we have tried to propagate the experimentally recovered part of semi-empirical DMF on larger interatomic interval $r \in [0.8, 1.9]$ Å by adding into the global fitting procedure the experimental intensity ratios obtained 40 years ago [34,35] from spontaneous emission bands observed from the high vibratioinal levels with $v \leq 38$. Absolute absorption intensities recently obtained for very high 7-0 overtone [27] and sub-percent measurements achieved for 3-0 band [24] were also included in the fit, together with overall experimental absolute intensities previously selected in Ref. [17]. The asymptotically correct mass-invariant DMF for the $X^1\Sigma^+$ state of the CO molecule was determined in a fully analytical form for $r \in [0, +\infty]$ by smoothly expanding the empirical region on the appropriated *ab initio* data. The resulting semi-empirical DMF can be used, along with mass-invariant PEC [15], to upgrade rovibrational line lists for any isotopologues of the CO molecule up

to the dissociation threshold. The corresponding FOR-TRAN subroutine is provided in the Supplementary Material.

2. Input data

2.1. The experimental absolute and relative intensities

The main input set of the experimental data presently used is still based on the absolute intensity measurements available for the $v \leq 6$ levels of the most abounded $^{12}C^{16}O$ isotopologue and recommended in Ref. [17]. This dataset was complemented by recent absorption measurements of the 7-0 band [27] and sub-percent accurate measurements achieved for the 3-0 band [24].

In the present work we also intend to utilise the empirical transition moment moment ratios (TDMr) obtained in Refs. [34,35] from relative intensity ratios measured in the emission spectra from high vibrational levels with $v < 41$. To our the best knowledge, these relative intensity data have only been used once to derive the DMF in the original article [34] appeared 40 years ago. These TDMr data can be roughly categorised into two groups:

- The first one consists of the ratios determined as

$$\text{TDMr}(v) = \frac{\text{TDM}(v, v+2)}{\text{TDM}(v+1, v+2)} \tag{1}$$

Hereafter, $\text{TDM}(v', v)$ represents (see, Equation (8)) the transition dipole moment between ro-vibrational states with vibrational quantum numbers $v' = v - 1$ and $v' = v - 2$. For this group, $v \in [1-12, 17-35]$.

- The second group involves ratios defined as

$$\text{TDMr}(v) = \frac{\text{TDM}(v, v+3)}{\text{TDM}(v+2, v+3)}, \tag{2}$$

where $v \in [9-21, 23-35]$.

Thus, the TDMr(v)-values in the 2-nd group corresponding to vibrational transitions with $\Delta v = 3$, making them the pronounce weaker than those in the 1-st group, which consist of transitions with $\Delta v = 2$.

The final spectroscopic (experimental) dataset used in the present Direct-Fit-Method consists of 548 absolute TDM values extracted from experimental absorption intensities with $v' \in \{0, 7\}$, 3 direct (Stark) DMF measurements [13,36,37] and 45 TDM ratios [34]. All other experimental data (including the minor isotopologues), which were excluded from the fit, is listed, nevertheless, in the output file given in the Supplementary Materials.

2.2. The ab initio data

To propagate the semi-empirical DMF outside the inter-atomic distance covering by the experimental datasets above we have tried to use *ab initio* DMF points obtained in the framework of the state-of-art electronic structure calculations. The main drawback of the available *ab initio* results on the ground state of CO molecule that they are not uniformly accurate at all internuclear distances due to strong and rapid variation of the configuration decomposition of the electronic wavefunction as the *r* distance changes. The issue is illustrated in Figure 2, which depicts the contribution of configurations to the electronic wavefunction as a function of interatomic distance. Near the equilibrium, the electronic wavefunction consists predominantly of a single configuration, making *ab initio* calculations relatively straightforward, allowing robust methods like coupled cluster (for example CCSD(T)) to be applied [28]. As the interatomic distance increases, the electronic wavefunction, once predominantly one-configurational, decomposes into a manifold of configurations. Interestingly, the single configuration dominant near equilibrium completely vanishes at larger distances. Consequently, 'one-configurational' methods like the 'gold standard' CCSD(T) method fails at distances beyond 1.5 Å.

The challenge persists even when employing multi-configuration methods like MRCI and MR-AQCC. In this case, the rapidly changing manifold of configurations with respect to internuclear distance complicates the selection of a reference configuration space for MRCI-type metho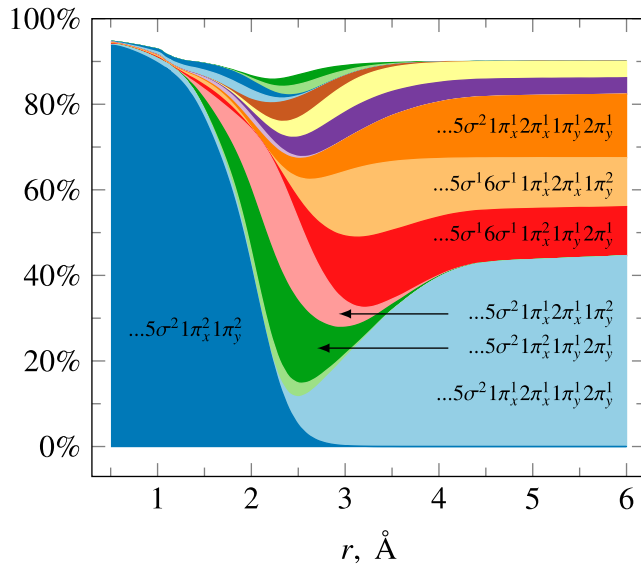ds. However, as the distance between atoms increases further, calculations become simpler since the wavefunction now consists of only a small number of dominant configurations with constant weights (see [31]). The plot shows this transition occurring for distances larger then 5 Å, marking the beginning of the long-range region, which starts beyond the so-called LeRoy radius (5.5 Å according to [31]). Remarkably, this plot allows estimation of the LeRoy radius without requiring more complex analyses of the long-range interatomic potential. Therefore, the domain spanning approximately 1.5 to 5.5 Å emerges as the toughest case for *ab initio* methods.

Nevertheless, the *ab initio* DMF data particularly included into the present fitting procedure consists of the MR-ACPF points borrowed from Ref.[17] which uniformly cover distances from 0.5 to 17 Å. These data are accompanied by a few DMF points evaluated near $r = 0$ in the framework of the united atom (UA) model [38].

3. An analytical form of semi-empirical DMF

To represent analytically the DMF function in the entire range of interatomic distances, the following model is employed:

$$d^{se}(r) = \frac{(1 - e^{-a_1 r})^7}{r^4}\left[\sum_{k=0}^{N} b_k T_k(z)\right], \quad (3)$$

where $T_k(z)$ are Chebyshev polynomials of the first kind and b_k are the linear expansion coefficients.

The mapping function used in Equation (3) non-linearly depends on the single parameter a_0:

$$z(r) = 1 - 2\,e^{-a_0 r}\left[1 + a_0 r\left(1 + \frac{1}{2}a_0 r\right)\right], \quad (4)$$

and transforms the infinite interval $r \in [0, +\infty)$ of the conventional radial coordinate r into the finite domain $z \in [-1, +1)$. The analytical transformation (4) ensures a higher density of the r-grid in the vicinity of the equilibrium distance r_e, where the wavefunctions of the lowest vibrational levels, which constitute the main body of experimental absolute intensity data, are localised (see, for details, appendix in Ref. [17]).

The $d^{se}(r)$ function defined by Equation (3) satisfies the physically justified asymptotic behaviour in both the united-atom (UA) and dissociation limits [31,38–41]:

$$d^{se}(r \to 0) = A_3 r^3; \quad d^{se}(r \to +\infty) = \frac{D_4}{r^4}, \quad (5)$$

where the short-range A_3 and long-range D_4 coefficients obey the constrains with the respect to the adjusted

Figure 2. The percentage contribution of configurations to which the electronic wave function of the ground state CO decomposes, depending on the inter-nuclear distance. Results are provided for the 16 configurations with the highest weights.

parameters of DMF:

$$A_3 = (a_1)^7 \left[\sum_{k=0}^{N} (-1)^k b_k \right]; \quad D_4 = \sum_{k=0}^{N} b_k. \quad (6)$$

It should be remind that the fully analytical form of the semi-empirical DMF (3) with the physically correct asymptotic behaviour at UA and dissociation limits is crucial to provide reliably transition probabilities for very weak vibrational bands until the highly excited levels [42–45].

4. A global least-squared fitting procedure

Both linear and non-linear parameters of the semi-empirical DMF, $d^{se}(r)$, were estimated iteratively by means of the weighted least-squares method by minimising the functional χ^2, which comprises the following three independent datasets:

$$\chi^2 = \chi^2_{tdm} + \chi^2_{rtdm} + \chi^2_{ab}, \quad (7)$$

where χ^2_{tdm} represents the sum of the squares of the residuals of experimental and calculated transition dipole moments (TDM) divided by the squares of their experimental uncertainties. Experimental TDM values were extracted from absolute intensities of absorption transitions using Eq.(15) from Ref. [17]. χ^2_{rtdm} is the same but for the TDM ratios whereas χ^2_{ai} is responsible for incorporating *ab initio* points.

It is clearly seen that uncertainties in the all input data are inevitably required to perform the weighted least squares fitting procedure. While uncertainties in experimental data are normally well-determined, uncertainties in their *ab initio* counterparts can be rather vague. Moreover, the latter estimates are not really statistical ones, which, if strictly speaking, should be used in the least squares method. In particular, the uncertainties of ACPF points estimated in Ref. [17] are mainly came due to the incompleteness of the basis set used, and they do not absorb the systematic error due to the insufficient number of electronic configurations used to take into account for the correlation effect.

In the original articles [34,35], the particular uncertainties of each TDMr are not specified, but an interval of 3-5% uncertainty is given for the entire set, except for the highest and lowest levels, where it can be reach 10%. Initially, an uncertainty of 3% was assigned to all TDMr values. The preliminary fit showed good agreement between experimental and calculated TDMr for the 1-st set, except for TDMr with $v \leq 3$ that have larger uncertainties, consistent with [34]. Since these TDMr do not affect very much on the DMF in the interval of r, which is governed

by more precise experimental data on absolute intensities available for $v \leq 7$, they were excluded from subsequent fits.

It should be noted that searching for the minimum of the χ^2 functional (7) with respect to the b_i coefficients on which the DMF depends linearly is not a big deal using the Levenberg–Marquardt algorithm [46]. At the same time, searching for the minimum with respect to two rest nonlinear parameters (a_0 and a_1) turns out to be a non-trivial task. In this case, χ^2 forms rather sophisticated 2D surface with several local minima, necessitating a thorough scan to find a global minimum. This highlights the importance of developing semi-empirical models that are linear with respect to a major number of fitting parameters.

The required theoretical TDM values $(v', J') \to (v'', J'')$ were calculated as

$$TDM_k^{se} = \int_0^\infty \psi_{v'J'}(r) \, d^{se}(r) \psi_{v''J''}(r) \, dr, \quad (8)$$

where $\psi_{vJ}(r)$ are properly normalised ro-vibrational wavefunctions of bound states. The required eigenvalues and eigenfunctions were obtained for each ro-vibrational bound level of the ground CO state by means of a numerical solution of the radial Schrödinger equation with the highly accurate semi-empirical PEC (see [15] for details).

5. Results and discussion

The fitted parameters of the semi-empirical DM function defined by Equation (3) are given on the Table 1. The relevant covariance matrix is provided in the Supplementary Material. An interesting property of the present fit corresponding to the global minimum searching of the functional (7) is that it leads to alternating sign b_k-coefficients in the Chebyshev polynomial expansion of the DMF. The quality of the fit across various data types included in the fitting procedure is represented by the dimensionless root-mean-square deviation, calculated as $\overline{dd} = \sqrt{\chi^2/N}$, and presented in Table 2. The short-range coefficient A_3 computed with the present DMF is 864 DÅ^{-3}, compared to the 1005 DÅ^{-3} estimated in [38]. The obtained value of the long-range coefficient $D_4 \approx -5.15$ DÅ^4, aligns well with the *ab initio* estimate of -5.1 ± 0.1 DÅ^4 [31], which was derived using only atomic data.

The Figure 3 illustrates the present DM curve alongside several others from the literature, focusing on the most challenging range of internuclear distances where experimental data is lacking and *ab initio* methods are apparently to fail. Noticeable distinctions among the curves emerge beyond $r > 1.6$ Å, marking the end of the main experimental TDM data's influence. The present DMF closely aligns with the Chackerian et al. curve up to

Table 1. The resulting fitted parameters of the present semi-empirical DMF defined by Equation (3) for the CO ground state. Two non-linear parameters a_0 and a_1 are both given in 1/Å, while the linear expansion coefficients b_i in DÅ^4. The FORTRAN subroutine generating the present DMF is given in the Supplementary Material.

a_0	2.93767
a_1	0.76042
b_0	588.66060
b_1	−1095.24464
b_2	1163.00881
b_3	−1020.26040
b_4	755.18055
b_5	−566.96168
b_6	329.26551
b_7	−208.85637
b_8	89.53594
b_9	−46.60804
b_{10}	11.64195
b_{11}	−4.51507

Table 2. Dimensionless root-mean-square deviation $(\overline{dd})$ for each type of input data.

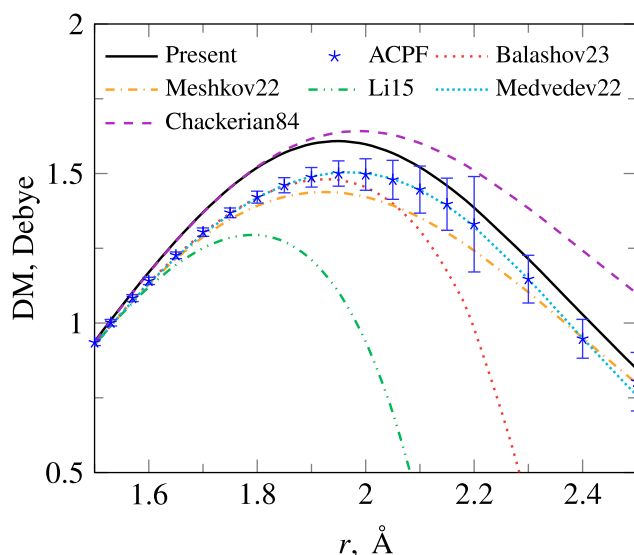| Input data	$\overline{dd}$
TDM (multiple sources)	0.49
TDMr [34]	0.47
UA [38]	0.67
MR-ACPF [17]	0.41

Figure 3. Present semi-empirical DMF (solid line), *ab initio* points calculated by MR-ACPF method [17] and previous DM functions borrowed from different sources [16–18,27,34]. The error bars of *ab initio* points represent uncertainties estimated in Ref. [17].

1.85 Å, where both functions are influenced by intensity ratio data (TDMr). Beyond this point, the curves begin to diverge as the impact of TDMr values diminishes. This divergence occurs near the right turning point at $r = 1.93$ Å for the vibrational level with $v = 38$, which is the last level contributing to intensity ratios set. Thereafter, the present curve gradually converges towards the *ab initio*
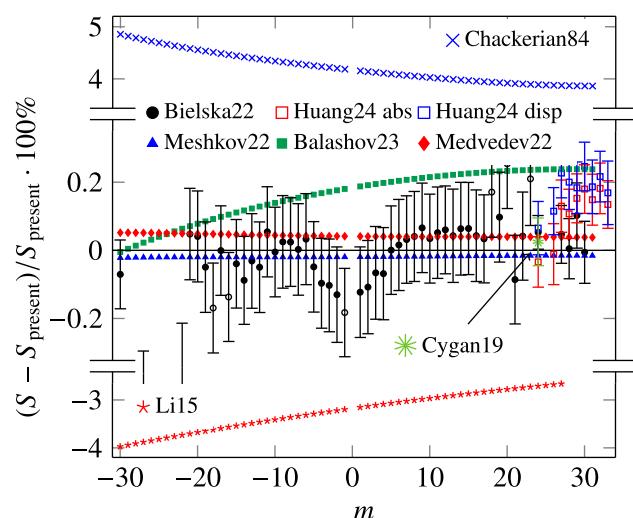

Figure 4. Relative differences between intensities calculated with the present DM function and both experimental data [23,25,27] and intensities computed using DM functions from previous studies [16–18,27]. The error bars represent experimental uncertainties reported in [23,25,27]. Experimental intensities not included in the fitting procedure are depicted with unfilled marks.

points. However, it has been elucidated that including MR-ACPF points from the interval $r \in [1.4, 2.5]$ Å in the fitting procedure deteriorates the reproduction of experimental data (mainly TDMr values). This may be due to flaws in the *ab initio* data itself, the experimental data, or both. The DM curves relying on relative intensities instead of *ab initio* data demonstrate a higher maximum, with deviations exceeding the systematic uncertainties of *ab initio* points estimated in [17], which account only for basis set incompleteness and not the correlation error of the method itself.

The Figure 4 demonstrates how the present DMF reproduces recent sub-percent accurate line-intensity measurements of the 3-0 band [23–25]. It also compares these results with previous estimates. The quality of the fit of the main data from Ref. [24] is $\overline{dd} = 0.54$. This value does not account for several obvious outliers in the experimental data that were not included in the fitting procedure. When considering all measured intensities $\overline{dd} \approx 1.05$. The 3-0 band data from Ref. [25], which only cover a restricted range of $25 \leq J \leq 34$, show a systematic overestimation from our results and do not align well with the data from [24]. Consequently, these data were excluded from the final fitting procedure. Remarkably, the predictions from our previous study [17] and also from [18] show strong alignment with the present results, despite not directly incorporating the sub-percent measurements from [24]. It's noteworthy that both semi-empirical DMFs relied solely on a single high-precision line measurement from [23]. However, including this point is happen to be significant to
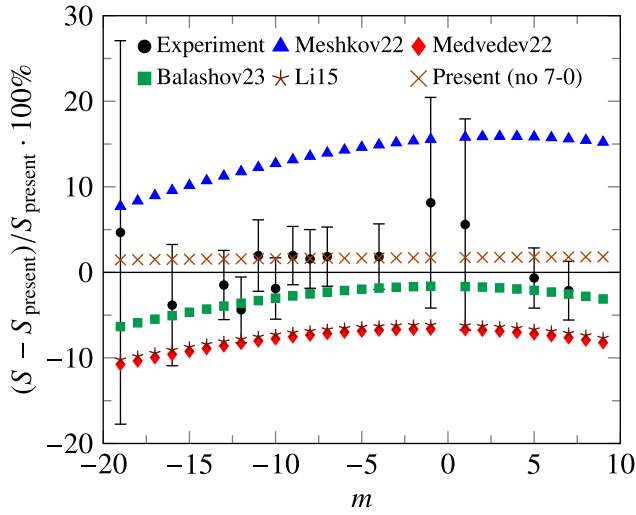
Figure 5. Comparison of line intensities of the $^{12}C^{16}O$ 7-0 band, calculated using the current DMF, with experimental values [27] and values computed using DMF obtained from [16–18,27]. The error bars represent experimental uncertainties reported in [27].

improve overall predictions across the entire band due to its extremely small uncertainty. The Figure 5 illustrates the relative deviations between the intensities of the 7-0 band calculated with the present DMF and experimental measurements, alongside results from previous studies. The current DMF yields $\overline{dd} \approx 0.57$. Calculations using the DM functions from previous studies, which do not include the 7-0 band data [16–18], show a deviation of about 10-15% from the experimental data, slightly exceeding the bounds of experimental uncertainty. Notably, the simple polynomial model proposed by Li at al. [16] provides an even better prediction of the 7-0 band than the more complex DMFs from [17] and [18]. The DMF from [27], which is based on the alternative *ab initio* MR-CISD-Q-FF data, shows good agreement with the experiment, but it should not be regarded as predictive for the 7-0 band because the experimental intensities were used to select appropriate *ab initio* points, which were then approximated by a polynomial. The label 'present (no 7-0)' on Figure 5 denotes a test calculation where all data, except for the 7-0 intensities, are included in the fitting procedure. The resulting DMF yields intensities closer to the experimental values than both DMFs from [17,18]. This result may be attributed to the exclusion of apparently corrupted data for the 5-0 band, which could affect predictions for the 7-0 band. It is also worth noting that including relative intensities doesn't negatively affect the 7-0 band predictions. Since the main aspect of this work is the addition of experimental data on intensity ratios, it is interesting to see how these ratios are reproduced with the resulting DMF. The 1-st set, which consists of transitions with $\Delta v = 2$, is depicted in the upper graph of Figure 6. The present
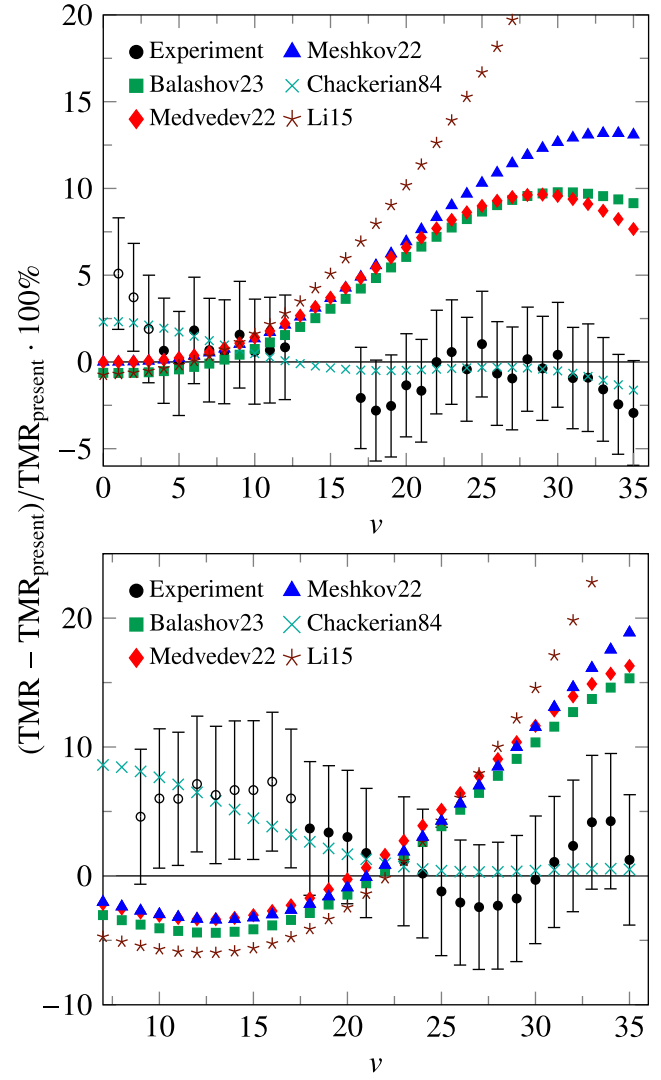

Figure 6. Comparison of TDM ratios, calculated using the present DMF, with empirical values from [34], and those computed using DMFs obtained from [16,17,27,34]. The TDMr in the upper plot are defined by Equation (1), while those in the lower plot by Equation (2). Experimental TDMr values not included in the fitting procedure are depicted with unfilled marks.

DMF represents this set with $\overline{dd} \approx 0.7$, demonstrating the same quality as the original DMF of Chackerian at al. [34], which is based almost solely on this data. Notably, this set of TDMr intersects with the main set of TDM data (for $v \leq 7$) and appears fully compatible with it, except for outliers with $v \leq 3$.

The 2-nd dataset, consisting of transitions with $\Delta v = 3$, is shown in the lower graph. For levels with $v \leq 17$, a systematic deviation larger than their uncertainty is observed, leading to their escape from the fitting process. The remaining levels exhibit a good agreement between experimental and calculated values. For the 2-nd set of TDMr, a group of outliers emerged within the v range of 9-17, showing deviations slightly exceeding 5%, which is beyond the stated range of uncertainties. This could be attributed to these TDMr having the lowest

absolute values (which increase with v), making them more susceptible to measurement or processing issues. These TDMr were excluded from subsequent fits. The uncertainty for the remaining TDMr in the second set was then increased to 5%, the maximum value reported in [34].

6. Concluding remarks

The semi-empirical mass-invariant dipole moment function (DMF) for the ground state of the CO molecule was redefined in the analytical form by a weighed non-linear least-squared fitting both absolute and relative experimental intensities available up to $v \le 38$ vibrational levels, excluding 'abnormally' weak 5-0 band, particular outliers and data related to all minor isotopologues. Absolute absorption intensities recently obtained for very high 7-0 overtone and accompanied sub-percent measurements for 3-0 band were also included in the fitting procedure. The region $r \in [0.8, 1.9]$ Å expanded exclusively by the empirical relative intensity data was propagated into the entire range of interatomic distances by adding of the selected *ab initio* points. Specifically, a few points coming from the UA model provided the information on the DMF near $r = 0$, while MR-ACPF points at the long-range distance $r > 5.5$ Å ensured the correct $1/r^4$ asymptotic behaviour at $r \to +\infty$.

The present DMF reproduces a vast majority of the experimental intensities within accuracy of measurements, and, hence, can be recommended, in a combination with a highly accurate interatomic PEC, to upgrade ro-vibrational line lists for any CO isotopologue up to the dissociation threshold. The corresponding FORTRAN subroutine is provided in the Supplementary Material. For instance, the radiative lifetimes $\tau(v)$ systematically predicted for all bound vibrational levels of the $X^1\Sigma^+$ state of the major $^{12}C^{16}O$ isotopologue are depicted on Figure 7. The resulting $\tau(v)$-values demonstrate a shallow minimum for the intermediate v-levels, and, numerically confirm the mentioned importance of DMF reconstruction in analytical form with physically correct asymptotic behaviour.

It has been unambiguously found out that the absolute intensities measured for 5-0 band cannot be fitted well together with the intensity ratios. That is, it turns out that from the experimental data on absolute intensities only 5-0 band is incompatible with intensity ratios measured in [34]. The 'suspicious' 5-0 measurements of the single work [47] seem to be revisited with more sensitive techniques due to their low signal-to-noise ratio. The 5-0 theoretical probabilities also was proved to be the extremely sensitive to any systematic variation of DMF and PEC [44,45].
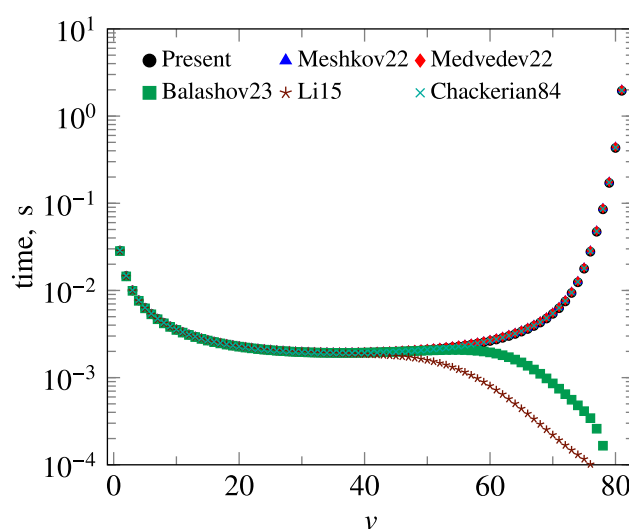

Figure 7. Comparison of radiative lifetimes $\tau(v)$ calculated for all bound vibration levels with $0 \le v \le 81$ and $J = 1$ using the present and previous DMFs [16–18,27,34].

The present semi-empirical DMF systematically overestimates the most *ab initio* curves available at $r \ge 1.6$ Å. A closer examination of these data led to the conclusion that they could be particularly inaccurate for interatomic distances from 1.6 to 5.5 Å. In summary, the present work highlights the need for a thorough theoretical investigation of both dipole DMF and PEC in the range $r \in [1.5, 5.5]$ Å by means of multi-reference *ab initio* methods which are able to comprehensively accounted for electronic correlation effect. Overall, a robust CO DMF is still a challenge for both experimental and *ab initio* approaches.

Disclosure statement

No potential conflict of interest was reported by the author(s).

References

[1] P. Bernath, J. Quant. Spectrosc. Rad. Transf. **186**, 3–16 (2017). doi:10.1016/j.jqsrt.2016.04.006, Satellite Remote Sensing and Spectroscopy: Joint ACE-Odin Meeting, October 2015.
[2] C.A. Beale, E.M. Buzan, C.D. Boone, P.F. Bernath and J. Mol, Spectrosc. **323**, 59–66 (2016).

[3] C. Abia, S. Palmerini, M. Busso and S. Cristallo, Astron. Astrophys. **548**, A55 (2012). doi:10.1051/0004-6361/201220148

[4] T. Delahaye, R. Armante, N.A. Scott, N. Jacquinet-Husson, A. Chédin, L. Crépeau, C. Crevoisier, V. Douet, A. Perrin, A. Barbe, V. Boudon, A. Campargue, L.H. Coudert, V. Ebert, J.M. Flaud, R.R. Gamache, D. Jacquemart, A. Jolly, F. Kwabia Tchana, A. Kyuberis, G. Li, O.M. Lyulin, L. Manceron, S. Mikhailenko, N. Moazzen-Ahmadi, H.S. Müller, O.V. Naumenko, A. Nikitin, V.I. Perevalov, C. Richard, E. Starikova, S.A. Tashkun, V.G. Tyuterev, J. Vander Auwera, B. Vispoel, A. Yachmenev, S. Yurchenko and J. Molec, Spectrosc. **380**, 111510 (2021).

[5] P. Giacobbe, M. Brogi, S. Gandhi, P.E. Cubillos, A.S. Bonomo, A. Sozzetti, L. Fossati, G. Guilluy, I. Carleo, M. Rainer, A. Harutyunyan, F. Borsa, L. Pino, V. Nascimbeni, S. Benatti, K. Biazzo, A. Bignamini, K.L. Chubb, R. Claudi, R. Cosentino, E. Covino, M. Damasso, S. Desidera, A.F.M. Fiorenzano, A. Ghedina, A.F. Lanza, G. Leto, A. Maggio, L. Malavolta, J. Maldonado, G. Micela, E. Molinari, I. Pagano, M. Pedani, G. Piotto, E. Poretti, G. Scandariato, S.N. Yurchenko, D. Fantinel, A. Galli, M. Lodi, N. Sanna and A. Tozzi, Nature **592**, 205–208 (2021). doi:10.1038/s41586-021-03381-x

[6] K.S. Olsen, F. Lefèvre, F. Montmessin, A.A. Fedorova, A. Trokhimovskiy, L. Baggio, O. Korablev, J. Alday, C.F. Wilson, F. Forget, D.A. Belyaev, A. Patrakeev, A.V. Grigoriev and A. Shakun, Nat. Geosci. **14**, 67–71 (2021). doi:10.1038/s41561-020-00678-w

[7] Y.V. Pavlenko, S.N. Yurchenko and J. Tennyson, Astron. Astrophys. **633**, A52 (2020). doi:10.1051/0004-6361/201936811

[8] J. Veefkind, I. Aben, K. McMullan, H. Förster, J. de Vries, G. Otter, J. Claas, H. Eskes, J. de Haan, Q. Kleipool, M. van Weele, O. Hasekamp, R. Hoogeveen, J. Landgraf, R. Snel, P. Tol, P. Ingmann, R. Voors, B. Kruizinga, R. Vink, H. Visser and P. Levelt, Remote. Sens. Environ. **120**, 70–83 (2012). doi:10.1016/j.rse.2011.09.027

[9] A.C. Vandaele, A. Mahieux, S. Chamberlain, B. Ristic, S. Robert, I.R. Thomas, L. Trompet, V. Wilquet and J.L. Bertaux, Icarus **272**, 48–59 (2016). doi:10.1016/j.icarus.2016.02.025

[10] J.R. Lyons, E. Gharib-Nezhad and T.R. Ayres, Nat. Commun. **9**, 908 (2018). doi:10.1038/s41467-018-03093-3

[11] P. De Biévre, M. Gallet, N.E. Holden and I.L. Barnes, J. Phys. Chem. Ref. Data **13**, 809–891 (1984). doi:10.1063/1.555720

[12] D.I. Pineda, F.A. Bendana, K.K. Schwarm and R.M. Spearrin, Combust. Flame. **207**, 379–390 (2019). doi:10.1016/j.combustflame.2019.05.030

[13] J.F. Ogilvie, S.L. Cheah, Y.P. Lee and S.P.A. Sauer, Theor. Chem. Acc. **108**, 85–97 (2002). doi:10.1007/s00214-002-0337-y

[14] J.A. Coxon and P.G. Hajigeorgiou, J. Chem. Phys. **121**, 2992–3008 (2004). doi:10.1063/1.1768167

[15] V.V. Meshkov, A.V. Stolyarov, A. Yu. Ermilov, E.S. Medvedev, V.G. Ushakov, I.E. Gordon and J. Quant, Spectrosc. Radiat. Transf. **217**, 262–273 (2018). doi:10.1016/j.jqsrt.2018.06.001

[16] G. Li, I.E. Gordon, L.S. Rothman, Y. Tan, S.M. Hu, S. Kassi, A. Campargue and E.S. Medvedev, Astrophys. J. Suppl. Ser. **216**, 15 (2015). doi:10.1088/0067-0049/216/1/15

[17] V.V. Meshkov, A.Y. Ermilov, A.V. Stolyarov, E.S. Medvedev, V.G. Ushakov and I.E. Gordon, J. Quant. Spectrosc. Radiat. Transf. **280**, 108090 (2022). doi:10.1016/j.jqsrt.2022.108090

[18] E.S. Medvedev and V.G. Ushakov, J. Quant. Spectrosc. Radiat. Transf. **288**, 108255 (2022). doi:10.1016/j.jqsrt.2022.108255

[19] I.E. Gordon, L.S. Rothman, C. Hill, R.V. Kochanov, Y. Tan, P.F. Bernath, M. Birk, V. Boudon, A. Campargue, K.V. Chance, B.J. Drouin, J.M. Flaud, R.R. Gamache, J.T. Hodges, D. Jacquemart, V.I. Perevalov, A. Perrin, K.P. Shine, M.A.H. Smith, J. Tennyson, G.C. Toon, H. Tran, V.G. Tyuterev, A. Barbe, A.G. Császár, V.M. Devi, T. Furtenbacher, J.J. Harrison, J.M. Hartmann, A. Jolly, T.J. Johnson, T. Karman, I. Kleiner, A.A. Kyuberis, J. Loos, O.M. Lyulin, S.T. Massie, S.N. Mikhailenko, N. Moazzen-Ahmadi, H.S.P. Müller, O.V. Naumenko, A.V. Nikitin, O.L. Polyansky, M. Rey, M. Rotger, S.W. Sharpe, K. Sung, E. Starikova, S.A. Tashkun, J.V. Auwera, G. Wagner, J. Wilzewski, P. Wcisło, S. Yu and E.J. Zak, J. Quant. Spectrosc. Radiat. Transf. **203**, 3–69 (2017). doi:10.1016/j.jqsrt.2017.06.038

[20] I.E. Gordon, L.S. Rothman, R.J. Hargreaves, R. Hashemi, E.V. Karlovets, F.M. Skinner, E.K. Conway, C. Hill, R.V. Kochanov, Y. Tan, P. Wcisło, A.A. Finenko, K. Nelson, P.F. Bernath, M. Birk, V. Boudon, A. Campargue, K.V. Chance, A. Coustenis, B.J. Drouin, J.M. Flaud, R.R. Gamache, J.T. Hodges, D. Jacquemart, E.J. Mlawer, A.V. Nikitin, V.I. Perevalov, M. Rotger, J. Tennyson, G.C. Toon, H. Tran, V.G. Tyuterev, E.M. Adkins, A. Baker, A. Barbe, E. Canè, A.G. Császár, A. Dudaryonok, O. Egorov, A.J. Fleisher, H. Fleurbaey, A. Foltynowicz, T. Furtenbacher, J.J. Harrison, J.M. Hartmann, V.M. Horneman, X. Huang, T. Karman, J. Karns, S. Kassi, I. Kleiner, V. Kofman, F. Kwabia–Tchana, N.N. Lavrentieva, T.J. Lee, D.A. Long, A.A. Lukashevskaya, O.M. Lyulin, V.Y. Makhnev, W. Matt, S.T. Massie, M. Melosso, S.N. Mikhailenko, D. Mondelain, H.S.P. Müller, O.V. Naumenko, A. Perrin, O.L. Polyansky, E. Raddaoui, P.L. Raston, Z.D. Reed, M. Rey, C. Richard, R. Tóbiás, I. Sadiek, D.W. Schwenke, E. Starikova, K. Sung, F. Tamassia, S.A. Tashkun, J. Vander Auwera, I.A. Vasilenko, A.A. Vigasin, G.L. Villanueva, B. Vispoel, G. Wagner, A. Yachmenev and S.N. Yurchenko, J. Quant. Spectrosc. Radiat. Transf. **277**, 107949 (2021). doi:10.1016/j.jqsrt.2021.107949

[21] L.S. Rothman, I.E. Gordon, R.J. Barber, H. Dothe, R.R. Gamache, A. Goldman, V.I. Perevalov, S.A. Tashkun and J. Tennyson, J. Quant. Spectrosc. Radiat. Transf. **111**, 2139–2150 (2010). doi:10.1016/j.jqsrt.2010.05.001

[22] H. Lefebvre-Brion and R.W. Field, *The Spectra and Dynamics of Diatomic Molecules: Revised and Enlarged Edition*, ELSEVIER Academic Press (Amsterdam-Boston-Heidelberg-London-New York-Oxford-Paris-San Diego-San-Francisco-Singapure-Sydney-Tokyo), (2004).

[23] A. Cygan, P. Wcisło, S. Wójtewicz, G. Kowzan, M. Zaborowski, D. Charczun, K. Bielska, R.S. Trawiński, R. Ciuryło, P. Masłowski and D. Lisak, Opt. Express. **27**, 21810 (2019). doi:10.1364/OE.27.021810

[24] K. Bielska, A.A. Kyuberis, Z.D. Reed, G. Li, A. Cygan, R. Ciuryło, E.M. Adkins, L. Lodi, N.F. Zobov, V. Ebert, D. Lisak, J.T. Hodges, J. Tennyson and O.L. Polyansky, Phys. Rev. Lett. **129**, 043002 (2022). doi:10.1103/PhysRevLett.129.043002

[25] Q. Huang, Y. Tan, R.H. Yin, Z.L. Nie, J. Wang and S.M. Hu, Line intensities of CO near 1560 nm measured with absorption and dispersion spectroscopy 2024.

[26] A.O. Lykhin, D.G. Truhlar and L. Gagliardi, J. Chem. Theory Comp. **17**, 7586–7601 (2021). doi:10.1021/acs.jctc.1c00915

[27] A.A. Balashov, K. Bielska, G. Li, A.A. Kyuberis, S. Wójtewicz, J. Domyslawska, R. Ciurylo, N.F. Zobov, D. Lisak, J. Tennyson and O.L. Polyansky, J. Chem. Phys. **158** (23), 234306 (2023). doi:10.1063/5.0152996

[28] D.P. Usov, Y.S. Kozhedub, V.V. Meshkov, A.V. Stolyarov, N.K. Dulaev, A.M. Ryzhkov, I.M. Savelyev, V.M. Shabaev and I.I. Tupitsyn, Phys. Rev. A. **109**, 042822 (2024). doi:10.1103/PhysRevA.109.042822

[29] V. Špirko, J. Chem. Theory. Comput. **20** (11), 4711–4717 (2024). doi:10.1021/acs.jctc.4c00098

[30] E. Konovalova, Y. Demidov and A. Stolyarov, Opt. Spectrosc. **125**, 470–475 (2018). doi:10.1134/S0030400X18100107

[31] V.G. Ushakov, V.V. Meshkov, A. Yu. Ermilov, A.V. Stolyarov, I.E. Gordon and E.S. Medvedev, Phys. Chem. Chem. Phys. **22**, 12058–12067 (2020). doi:10.1039/D0CP01696A

[32] H.J. Chen, J. Wu, H. Liu and X.L. Cheng, Chin. Phys. B. **24**, 083102 (2015). doi:10.1088/1674-1056/24/8/083102

[33] V.V. Meshkov, E.A. Pazyuk, A.V. Stolyarov, D.P. Usov, A.M. Ryzhkov, I.M. Savelyev, Y.S. Kozhedub, N.S. Mosyagin and V.M. Shabaev, Russ. J. Phys. Chem. A. **97** (10), 2165–2170 (2023). doi:10.1134/S0036024423100163

[34] C. Chackerian Jr, R. Farrenq, G. Guelachvili, C. Rossetti and W. Urban, Canad. J. Phys. **62**, 1579–1585 (1984). doi:10.1139/p84-202

[35] R. Farrenq, C. Rossetti, G. Guelachvili and W. Urban, Chem. Phys. **92** (2-3), 389–399 (1985). doi:10.1016/0301-0104(85)85033-3

[36] J.S. Muenter, J. Mol. Spectrosc. **55**, 490–491 (1975). doi:10.1016/0022-2852(75)90287-8

[37] M. Birk, D. Hausamann, G. Wagner and J.W. Johns, Appl. Opt. **35**, 2971–2985 (1996). doi:10.1364/AO.35.002971

[38] M.A. Buldakov, V.N. Cherepanov, E.V. Koryukina and Yu. N. Kalugina, J. Phys. B: At. Mol. Opt. Phys. **42**, 105102 (2009). doi:10.1088/0953-4075/42/10/105102

[39] J. Goodisman, J. Chem. Phys. **38**, 2597–2599 (1963). doi:10.1063/1.1733557

[40] M.A. Buldakov, E.V. Koryukina, V.N. Cherepanov and Y.N. Kalugina, Phys. Rev. A. **78**, 032516 (2008). doi:10.1103/PhysRevA.78.032516

[41] M.A. Buldakov, V.N. Cherepanov and E.V. Koryukina, J. Phys. B: At. Mol. Opt. Phys. **42**, 185101 (2009). doi:10.1088/0953-4075/42/18/185101

[42] E.S. Medvedev, V.V. Meshkov, A.V. Stolyarov and I.E. Gordon, J. Chem. Phys. **143**, 154301 (2015). doi:10.1063/1.4933136

[43] E.S. Medvedev, V.V. Meshkov, A.V. Stolyarov, V.G. Ushakov and I.E. Gordon, J. Mol. Spectrosc.**330**, 36–42 (2016). doi:10.1016/j.jms.2016.06.013

[44] E.S. Medvedev, V.G. Ushakov, A.V. Stolyarov and I.E. Gordon, J. Chem. Phys. **147**, 164309 (2017). doi:10.1063/1.5000717

[45] E.S. Medvedev and V.G. Ushakov, J. Mol. Spectrosc. **349**, 60–63 (2018). doi:10.1016/j.jms.2018.04.008

[46] W.H. Press, S.A. Teukolsky, W.T. Vetterling and B.P. Flannery, *Numerical Recipes in FORTRAN: The Art of Scientific Computing*, 3rd ed (Cambridge University Press, New York, 2007). p. 963.

[47] C.Y. Chung, J.F. Ogilvie and Y.P. Lee, J. Phys. Chem. A. **109**, 7854–7858 (2005). doi:10.1021/jp052035x

[48] H.J. Werner, P.J. Knowles, G. Knizia, F.R. Manby and M. Schütz, WIREs Comput. Mol. Sci. **2**, 242–253 (2012). doi:10.1002/wcms.v2.2

[49] H.J. Werner and P.J. Knowles, MOLPRO, 2012.1, a package of *ab initio* programs see.